Applied Energy 177 (2016) 227–238

Contents lists available at ScienceDirect

Applied Energy

journal homepage: www.elsevier.com/locate/apenergy

Thermal energy storage for low and medium temperature applications using phase change materials – A review

Jose Pereira da Cunha *, Philip Eames

Centre for Renewable Energy Systems Technology (CREST), Loughborough University, Loughborough (Leicestershire) LE11 3TU, United Kingdom

HIGHLIGHTS

- Characterization of Phase Change Materials with a phase change between 0 and 250 °C.
- Review of heating and cooling applications benefiting from a latent heat storage.
- Review of indirect latent heat storage containers for process heating applications.
- Review of heat transfer enhancement techniques to be used within the PCM.

ARTICLE INFO

Article history:
Received 23 February 2016
Received in revised form 5 May 2016
Accepted 14 May 2016
Available online 24 May 2016

Keywords:
Phase change materials
Thermal energy storage
Inorganic PCMs
Organic PCMs
Eutectic PCMs
Latent heat storage

ABSTRACT

A comprehensive review of phase change materials (PCMs) with phase transition temperatures between 0 and 250 °C is presented. From that review, organic compounds and salt hydrates seem more promising below 100 °C and eutectic mixtures from 100 to 250 °C.

Practical indirect heat exchanger designs for latent heat storage systems were also assessed and feasible heat enhancement mechanisms reviewed. The focus on this temperature range is due to potential CO_2 emissions reduction able to be achieved replacing conventional heating and cooling applications in the domestic, commercial and public administration sectors, which represented around a quarter of the UK's final energy consumption in 2015.

Contents

* Corresponding author.
E-mail addresses: j.pereira-da-cunha@lboro.ac.uk (J. Pereira da Cunha), p.c.eames@lboro.ac.uk (P. Eames).

http://dx.doi.org/10.1016/j.apenergy.2016.05.097
0306-2619/

1. Introduction

To date, the measures adopted to stabilize global temperature rise below the 2 °C target, are likely to be insufficient [1]. If this target is to be achieved, there must be an increased effort to decarbonize global energy consumption, which still relies heavily on fossil fuel sources.

Conventional heating and cooling in the domestic, commercial and public administration sectors had a combined natural gas and petroleum products consumption of around 25% of the UK's final energy consumption in 2014 [2]. The distribution per sector is presented in Fig. 1.

To reduce the CO_2 emissions in the domestic heating sector, heat pumps could be used as an alternative to current fossil fuel burning systems; however, their usage should the restricted to off peak times (between 22.00 and 07.00), in order not to greatly increase the UK's electrical grid peak demand [3], Fig. 2, with local heat storage being used to meet heat demand at other times.

The daily variation of CO_2 emissions per kW h of electricity consumed for the 15th of January and July of 2015 are presented in Fig. 2, values were obtained for the generation mix for the UK national grid and CO_2 emission factors applied similar to those estimated by Hawkes [4]. In order to match the CO_2 emissions associated with grid electricity to natural gas used for space heating (204.9 gCO_2/kW h [2]), the minimum coefficient of performance (COP) required for heat pumps is approximately 2.

The use of solar thermal systems is another potential way of reducing CO_2 emissions associated with space and water heating, effective thermal energy storage will be essential to address the mismatch between the intermittent solar heat supply and the heat demand [6,7].

Thermal energy storage can be achieved through 3 distinct ways: sensible; latent or thermochemical heat storage. Sensible heat storage relies on the material's specific heat capacity. Latent heat storage relies on the material's phase change enthalpy to store heat within a narrow temperature range, providing greater energy density [kW h_{th}/m^3] than that achievable with sensible heat storage over the same temperature gradient; however, volumetric expansions during the melting process can reach 10–15% for some materials. Thermochemical heat storage is more energetic than latent heat storage, but since it relies on adsorption/desorption or other chemical reactions, reaction kinetics and reactor design significantly determine their actual performance, and require distinct charging and discharging temperatures [8] (usually between 100 and 300 °C, depending on the reaction), having potential interest for interseasonal storage applications. Fig. 3A shows, heat storage capacity [kW h_{th}/m^3] of water sensible heat storage and 3 PCMs over a 20 °C temperature interval; the PCMs store around 2.5–6 times more energy than water. Fig. 3B compares thermochemical heat storage to a packed rock bed heat storage system; the hydration of the thermochemical compound can theoretically release 25 times more energy than what achievable with 40 °C of air temperature increase in a rock bed heat storage system, although temperatures up to 120 °C are required for dehydration of the salt hydrate; such thermochemical heat storage materials may prove to be suitable candidates for inter seasonal thermal energy storage.

Medium and large scale systems such as centralized cooling (absorption chillers [9–11]) and district heating networks [12,13], used commonly in hospitals, commercial centres and office buildings could also benefit from latent heat storage systems, when supplied by solar thermal collectors.

Another potential application for latent heat storage would be integration into solar thermal driven organic rankine cycles (ORC) [14]. The characterization of a compact ORC system for low grade transient solar energy conversion was made by [15], and it was concluded that adding latent heat thermal energy storage could potentially stabilize the system to short term weather irregularities (clouds, fog, etc.) or even depending on the storage size, be able to maintain daily production.

Latent heat energy storage may also have use in industry when integrated in some thermal batch processes, potentially reducing sensible heat losses in the heating and cooling process necessary to achieve optimum process temperatures [9], and allowing heat to be stored between cycles. Such batch processes can be found in most of the food and beverages industry (beer, milk, chocolate, cheese, coffee, canned food) and industrial drying processes. The possible integration of solar thermal collectors into some common industrial applications in Cyprus was presented by Kalogirou [16].

For nominal operation of latent heat storage systems, the PCM must have a relative high latent heat of fusion, stability in its molten state and be chemically inert with its enclosure. Another important requirement would be a low degree of subcooling; else their enhanced heat capacity won't be fully realised. One of the main properties of commonly used PCMs is their low thermal conductivity, usually between 0.2 and 0.7 [W/m K], requiring the use of complex heat exchanger geometries to obtain required heat transfer rates from latent heat storage containers. Conventional techniques to overcome the low heat transfer characteristic rates would be the used of metal fins [17]; however novel promising techniques such as carbon cloths [18], shape stabilized PCMs with graphite [19,20] microencapsulated-PCM slurries [21] and direct contact latent heat storage systems [22,23] can also be used to increase the global UA value of latent heat storage systems.

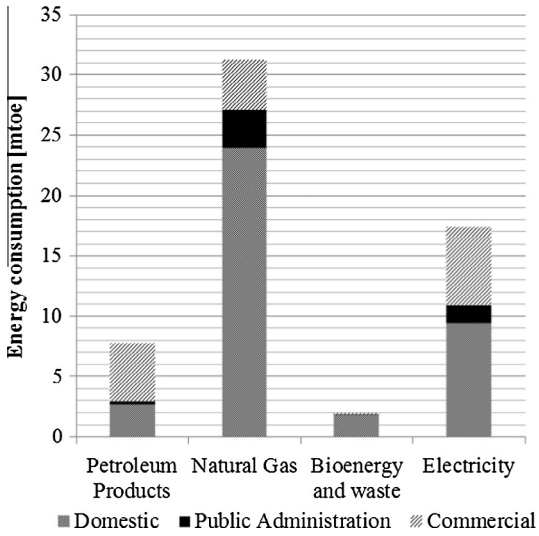

Fig. 1. The UK's final energy consumption aggregated values for 2014 [2] by source in the Domestic, Commercial and Public Administration sectors.

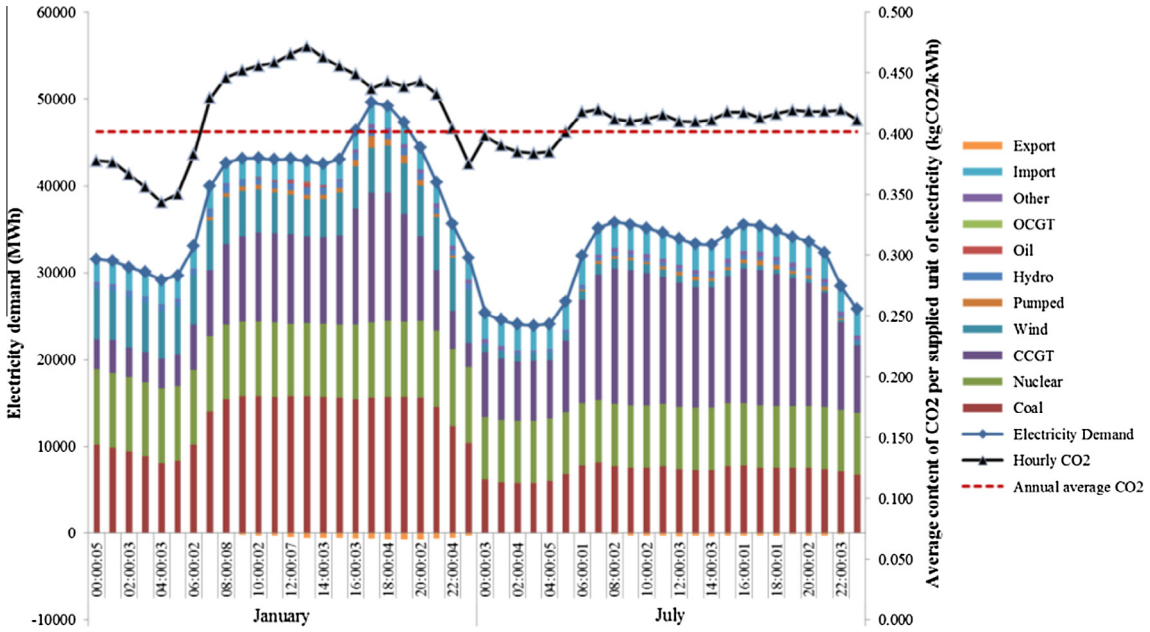

Fig. 2. Seasonal and hourly variation of CO_2 emissions associated with the electricity supplied by the UK national grid – sample date: 15/01/2015 & 15/07/2015 [4,5].

2. Phase change materials literature review

In order to assess the potential of latent heat storage applications, a comprehensive review of the PCMs physical properties during phase change is critical. For a comparative economic evaluation, market prices for industrial grade materials were used to provide a common approach.

2.1. Organic PCMs

Organic compounds, characterized by having carbon atoms in their structure, generally have very low thermal conductivity (from 0.1 to 0.7 W/m K), hence requiring mechanisms to enhance their heat transfer in order to achieve reasonable rates of heat output (W). Table 1 presents the thermophysical properties of the compounds identified for further analysis based on their relative low price, their quoted stability from the review and enthalpy of phase change. The Organic compounds reviewed that appeared to be promising in this temperature range are some of the saturated fatty acids [24]; sugar alcohols [25,26], carboxylic acids [27], amides [28] and alkanes [29]. Urea [30], is not a promising compound in its pure state, due to its instability when molten [31], but some of its eutectic mixtures seem to have suitable properties for latent heat storage, with details presented in Table 3.

2.2. Salt hydrates

Salt hydrates, formed by water absorption by the anhydrous salt at ambient temperatures, have a phase change enthalpy depending on the bond strength between the water molecules

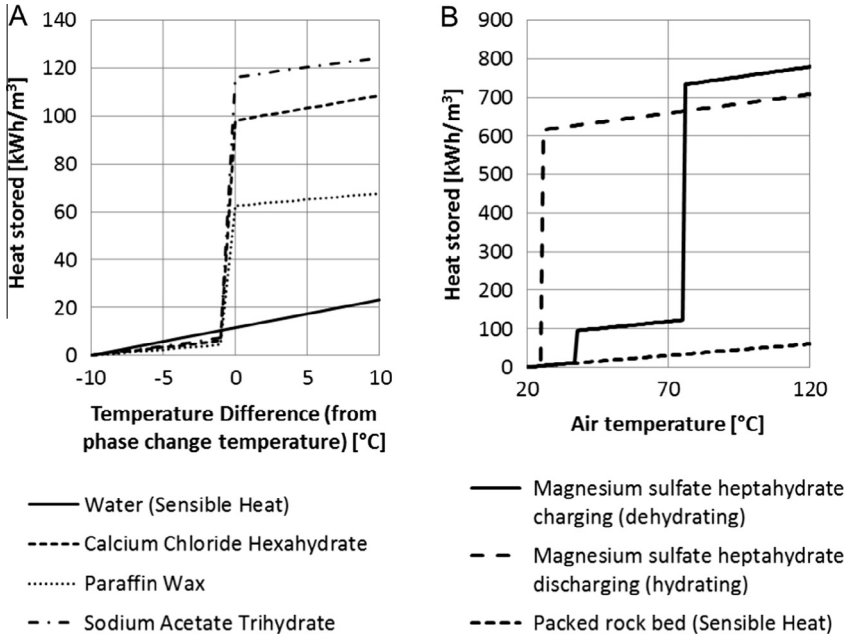

Fig. 3. Heat stored vs. temperature diagrams for 3 PCMs and a sensible water heat storage system (A) and magnesium sulphate heptahydrate (data retrieved from Zondag et al. [8]) compared to a conventional rock bed storage system (B).

Table 1
Thermophysical properties of selected organic compounds.

Compound	T_m	ΔH_m	Cp_s	Cp_l	λ_s	λ_l	ρ_s	V_{exp}	$E_{density}$	Price		Refs.
	°C	kJ/kg	kJ/kg K		W/m K		kg/m^3	m^3/m^3	kW h/m^3	£/m^3	£/kW h	
Formic acid	8	277	1.00	1.17	0.30	0.27	1227	12.0	96	255	4.2	[32,33]
Acetic acid	17	192	1.33	2.04	0.26	0.19	1214	13.5	71	327	7.2	[32,34]
Lauric acid	44	212	2.02	2.15	0.22	0.15	1007	13.6	66	276	6.5	[32,34]
Stearic acid	54	157	1.76	2.27	0.29	0.17	940	9.9	49	345	11.0	[31,33,35,36]
Palmitic acid	61	222	1.69	2.20	0.21	0.17	989	14.1	67	354	8.3	[32,35,37,38]
Paraffin wax	0–90	150–250	3.00	2.00	0.2		880–950	12–14	50–70	400–500	9.5–7.1	[9,32,39]
Acetamide	82	260	2.00	3.00	0.40	0.25	1160	13.9	93	1318	22.2	[32,40]
Oxalic acid	105	356	1.62	2.73			1900		211	524	3.9	[27,41]
Erythritol	117	340	2.25	2.61	0.73	0.33	1450	10.3	148	1287	13.6	[25,31,42]
HDPE	130	255	2.60	2.15	0.48	0.44	952		80	463	9.0	[32,43]
Phthalic anhydride	131	160	1.85	2.20			1530		85	2042	37.4	[44]
Urea	134	250	1.80	2.11	0.80	0.60	1320	16.7	97	189	3.0	[30,31,45]
Maleic acid	141	385	1.17	2.08			1590		184	1059	9.0	[31,46,47]
2-Chlorobenzoic acid	142	164	1.30	1.60			1544		83	1861	35.1	[48]
Adipic acid	152	275	1.87	2.72			1360	20.2	109	584	8.4	[49]
d-Mannitol	165	300	1.31	2.36	0.19	0.11	1490		139	1027	11.5	[25,50–52]
Hydroquinone	172	258	1.59	1.64			1300		105	3415	50.9	[32,53]

Table 2
Thermophysical properties of selected salt hydrates.

Compound	T_m	ΔH_m	Cp_s	Cp_l	λ_s	λ_l	ρ_s	V_{exp}	$E_{density}$	Price		Refs.
	°C	kJ/kg	kJ/kg K		W/m K		kg/m^3	m^3/m^3	kW h/m^3	£/m^3	£/kW h	
Water	0	333	3.30	4.18	1.60	0.61	920	−8.7	109	0	0.0	[32,57]
Calcium chloride hexahydrate	30	125	1.42	2.20	1.09	0.53	1710	11	64	93	2	[9,32,56,58]
Sodium sulphate decahydrate	32	180	1.93	2.80	0.56	0.45	1485	4	82	48	1	[9,32,56]
Sodium thiosulfate pentahydrate	46	210	1.46	2.39	0.76	0.38	1666	6	103	199	3	[32,43,59]
Sodium acetate trihydrate	58	266	1.68	2.37	0.43	0.34	1450	3	113	233	3	[32,60,61]
Barium hydroxide octahydrate	78	280	1.34	2.44	1.26	0.66	2180	11	171	422	4	[32,62,63]
Magnesium nitrate hexahydrate	89	140	2.50	3.10	0.65	0.50	1640	5	74	131	3	[9,32,54]
Oxalic acid dihydrate	105	264	2.11	2.89	0.90	0.70	1653	0	133	339	4	[31,41]
Magnesium chloride hexahydrate	117	150	2.00	2.40	0.70	0.58	1570	8	72	56	1	[32,54,64]

and the salt. Super cooling during crystallization [54], phase segregation [55] and corrosion with commonly used metals (copper, aluminium, stainless steel) [56], are the main issues inhibiting their use in latent heat energy storage systems. Table 2 presents the thermophysical properties for a selection of salt hydrates.

2.2.1. Phase separation

Water separation, related to poor molecular bonding [55,64] is the main factor determining thermal stability in the molten phase. Suitable encapsulation could help reduce the effects of water segregation, since it would prevent the release of partially evaporated water.

2.2.2. Super cooling

The onset of solidification can occur at a significantly lower temperature than the melting point, normally around 10–20 °C [37]. Adding other salts with similar crystal structures, increases nucleation points, and may reduce this phenomenon. A study of Magnesium chloride hexahydrate [64], proved that the addition of Strontium Carbonate, Strontium Hydroxide and Magnesium Hydroxide effectively reduced super cooling for this salt.

2.3. Eutectic PCMs

Binary and ternary mixtures of inorganic salts have been widely studied for thermal storage applications. Nitrate, chloride and sulphate salts of alkali and alkaline metals, such as magnesium, potassium, lithium and calcium, are the main compounds used to produce medium temperature eutectic mixtures, also known as ionic liquids [65].

Due to their higher density and stability in their liquid state, they have been used widely as ionic liquids in high temperature sensible thermal storage systems (thermonuclear energy, concentrated solar thermal power [66–68]).

Due to the lack of experimental data for some of the thermophysical properties of eutectic mixtures, weighting methods have been used to predict missing values [69,70]. More developed techniques to predict thermophysical properties of eutectic mixtures do exist [71,72], involving Van Der Waals volumes and surface areas of stable molecular combinations; however, more simplified correlations were used. The weighting correlations used to obtain the thermophysical properties, namely heat capacity (Cp), density (ρ), thermal conductivity (λ) and melting enthalpy (ΔH_m), are presented in Eqs. (1)–(6), which use available properties of the mixture and its constituents, molar ratio (x_i), mass ratio (w_i) and volumetric ratio (z_i) and their melting point (Tm) to predict the unknown values. A comparison was made with some eutectic salts for which experimental data was available; the difference between predictions and measurements was less than 10%. Table 3 presents the physical properties of the selected eutectic compounds in the 0–250 °C range, with the predicted latent heat values shown in bold.

$$w_i = x_i \times M_i \times \left(\sum_i x_i \times M_i\right)^{-1} \tag{1}$$

$$z_i = \frac{w_i}{\rho_i} \times \left(\sum_i \frac{w_i}{\rho_i}\right)^{-1} \tag{2}$$

$$Cp_{eutectic} = \sum_i Cp_i \times w_i \tag{3}$$

$$\rho_{eutectic} = \sum_i \rho_i \times z_i \tag{4}$$

$$\lambda_{eutectic} = \prod_i \lambda_i^{z_i} \tag{5}$$

$$\Delta H_{eutectic} = Tm_{eutectic} \times \sum_i \frac{\Delta H_i \times w_i}{Tm_i} \tag{6}$$

Table 3
Thermophysical properties of selected eutectic compounds.

Eutectic compounds	Mass ratio	T_m	ΔH_m	Cp_s	Cp_l	λ_s	λ_l	ρ_s	$E_{density}$	Price		Refs.
		°C	kJ/kg	J/kg K		mW/m K		kg/m^3	kW h/m^3	£/m^3	£/kW h	
$CaCl_2{\cdot}(H_2O)_6$ $MgCl_2{\cdot}(H_2O)_6$	67–33	25	**127**	1620	2270	**930**	**550**	1661	**57**	**80**	**1.4**	[32,43]
Urea $CH_3COONa{\cdot}(H_2O)_3$	60–40	30	**200**	1750	2210	**630**	**480**	1370	**74**	**206**	**2.8**	[43,73]
$Mg(NO_3)_2{\cdot}(H_2O)_6$ NH_4NO_3	61–39	52	**125**	2130	2670	**590**	**500**	1672	**58**	**188**	**3.3**	[43,73]
Urea–acetamide	38–62	53	**224**	1920	2660	**510**	**340**	1216	**73**	**924**	**13**	[58]
Stearic acid palmitic acid	36–64	53	182	1720	2230	234	169	971	46	351	8	[74]
$Mg(NO_3)_2{\cdot}(H_2O)_6$–$MgCl_2{\cdot}(H_2O)_6$	59–41	59	**132**	2290	2810	**670**	**530**	1610	**58**	**99**	**1.7**	[32,43]
Stearic acid –acetamide	83–17	65	**213**	1800	2400	**300**	**180**	972	**56**	**485**	**8.6**	
$LiNO_3$ $MgNO_3{\cdot}(H_2O)_6$	14–86	72	**180**	2380	2900	**700**	**510**	1713	**84**	**718**	**8.5**	
Urea–$LiNO_3$	82–18	76	218	1770	2020	850	600	1438	84	851	10.1	[73]
Urea–$NaNO_3$	71–29	83	187	1600	2030	750	590	1502	76	220	2.9	
Urea–NH_4Cl	85–15	102	214	1770	2090	760	580	1348	77	174	2.3	
Urea–K_2CO_3	15–85	102	206	1660	2020	780	580	1415	78	269	3.4	
Urea–KNO_3	77–23	109	195	1600	1910	810	580	1416	74	255	3.4	
Urea–NaCl	90–10	112	230	1720	2020	820	600	1372	85	180	2.1	
Urea–KCl	89–11	115	227	1690	1960	830	0.60	1370	83	197	2.4	
$LiNO_3$–$NaNO_3$–KNO_3	30–18–52	123	**140**	1170	1440	**790**	**530**	2068	**79**	**1979**	**25**	[75,76]
$LiNO_3$–KNO_3	34–66	133	**150**	1170	1350	**960**	**520**	2018	**82**	**2167**	**26**	[75–77]
KNO_3–$NaNO_2$	56–44	141	97	1180	1740	730	570	1994	52	504	9.7	78, p.778
KNO_3–$NaNO_3$–$NaNO_2$	53–6–41	142	**110**	1170	1730	**720**	**570**	2006	**60**	**497**	**8.3**	[32,78, p.786]
KNO_2–$NaNO_3$	48–52	149	124	1050	1630	580	520	2080	70	994	14	[78]
$LiNO_3$–$NaNO_2$	62–38	156	233	1570	1910	1120	660	2296	143	3816	27	
$LiNO_3$–KCl	58–42	160	**272**	1260	1350	**1310**	**590**	2196	**161**	**3409**	**21**	[32,79]
$LiNO_3$–$NaNO_3$–KCl	45–50–5	160	**266**	1320	1690	**880**	**590**	2297	**166**	**2852**	**17**	
HCOONa–HCOOK	45–55	176	175	1150	930	630	430	1913	92	421	4.6	[80]
LiOH–$LiNO_3$	19–81	183	352	1600	2000	1330	690	2124	202	5165	26	[78]
$LiNO_3$–$NaNO_3$	49–51	194	**262**	1350	1720	**870**	**590**	2317	**165**	**3084**	**19**	[32,78]
$LiNO_3$–NaCl	87–13	208	**369**	1540	1560	**1350**	**630**	2350	**235**	**5254**	**22**	[32,79,81]
KNO_3–KOH	80–20	214	83	1030	1350	880	540	1905	43	611	14	[32]
KNO_3–$NaNO_3$	55–45	222	**110**	1010	1490	**730**	**510**	2028	**61**	**482**	**8.0**	
LiBr–$LiNO_3$	27–73	228	279	1340	1380	1140	570	2603	196	6134	31	[78,82]
LiOH–$NaNO_3$–NaOH	6–67–27	230	**184**	1300	2000	**780**	**670**	2154	**107**	**538**	**5.0**	
$NaNO_2$–$NaNO_3$	55–45	233	**163**	1310	2130	**590**	**640**	2210	**97**	**382**	**3.9**	
$CaCl_2$–$LiNO_3$	13–87	238	317	1500	1530	1370	690	2362	204	5325	26	
LiCl–$LiNO_3$	9–91	244	342	1580	1610	1370	640	2351	218	6019	28	
$NaNO_3$–NaOH	86–14	250	**160**	1190	1860	**660**	**600**	2241	**97**	**339**	**3.5**	[32]

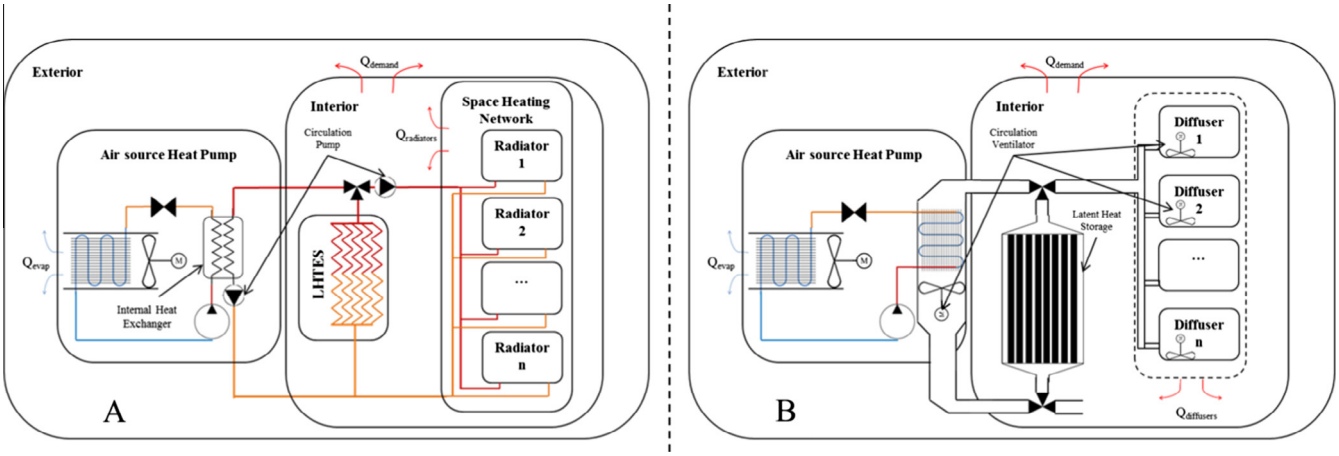

Fig. 4. Simplified diagrams of the integration of LHTES into water space heating systems (A) and centralized air space heating systems (B).

3. Potential applications for indirect latent heat storage containers and systems

The integration of latent heat storage containers into specific heating or cooling networks can be divided by the heat transfer fluid used: air or liquid. Using water as the heat transfer fluid, latent heat storage containers and systems could be integrated with conventional domestic central heating systems using water radiators, ideal to retrofit when changing a gas boiler for a heat pump [83], as illustrated in Fig. 4A. Using air as the heat transfer fluid, latent heat storage containers and systems can be integrated into centralized ventilation systems, typical in large office areas and commercial buildings, as illustrated in Fig. 4B.

Most latent heat storage containers can be divided into two groups: compact and encapsulated. In compact systems, the PCM is in enclosed within a large container with an embedded heat exchanger [84], a general configuration used is the shell and tube type, presented in Fig. 5A. Compact latent heat storage systems are generally designed to integrate with water heating systems [18,85]. Encapsulated systems are those in which the PCM is con-

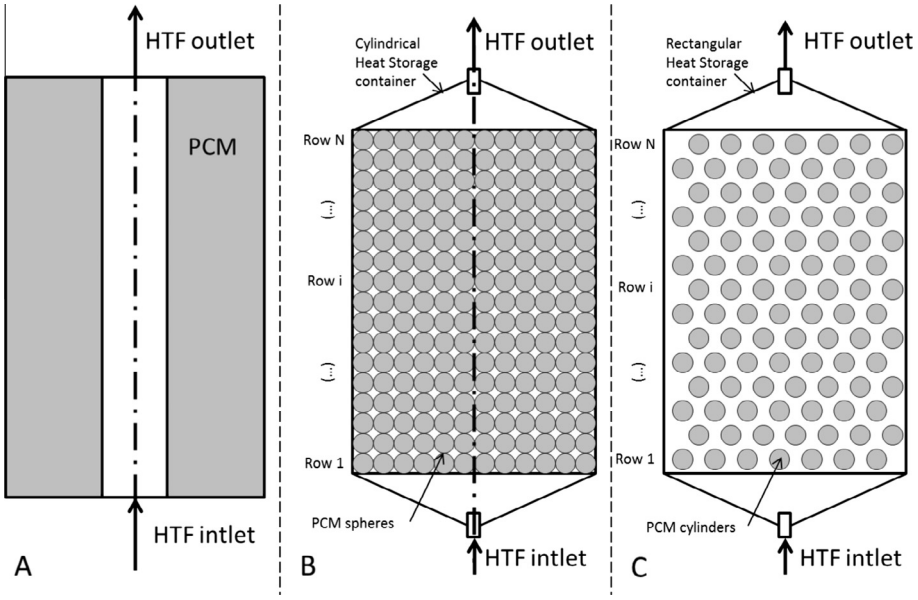

Fig. 5. Cross sections of a compact tube in tube (A), a encapsulated packed bed (B) and encapsulated staggered cylinders (C) latent heat storage containers.

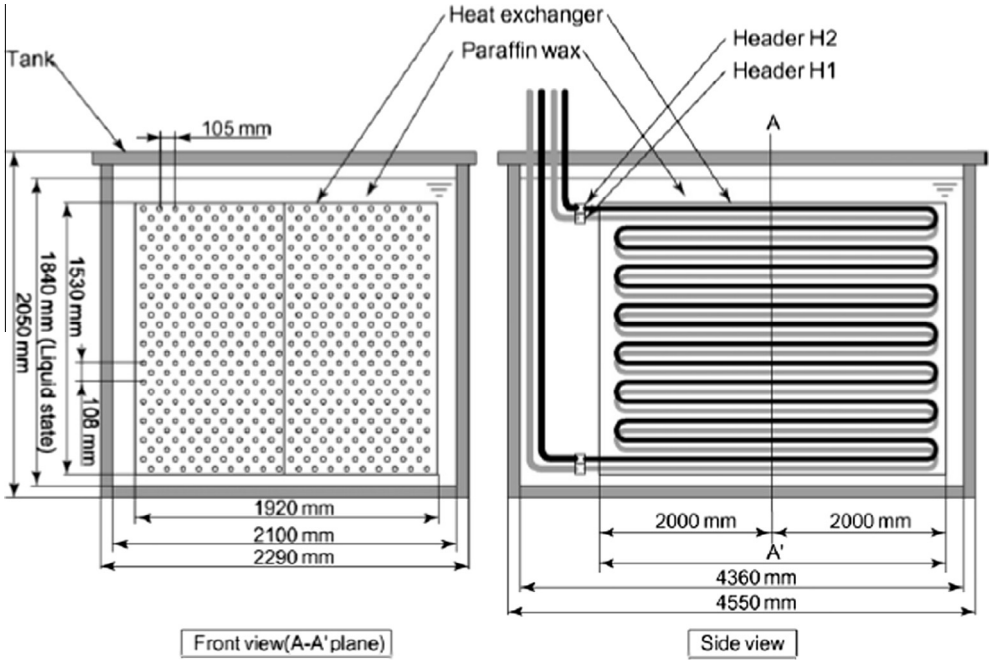

Fig. 6. A schematic diagram of the 18,770 L compact latent heat storage unit designed by Nakaso et al. [18], comprised of 18 parallel 28 mm copper tubes, each having 14 passes through the PCM volume.

tained within small containers, over which the heat transfer fluid flows, leading to a heat storage system that contains a greater component of sensible heat storage than compact latent heat storage systems over the same temperature range [86]. Such encapsulated designs have the versatility to be integrated with both air and water heating networks, due to their shape versatility and leak proof construction. Fig. 5 presents cross sections of a selection of 3 different types of latent heat storage containers suitable to be integrated with the heating networks described in Fig. 4. A void fraction needs to be included in the PCM storage container to allow for thermal expansion that occurs during the melt process.

3.1. Compact latent heat storage systems

Compact latent heat storage systems can have much higher PCM volumetric ratios [$m^3_{PCM}/m^3_{Container}$] than encapsulated latent heat systems, providing in theory longer duration isothermal outputs; however, low rates of thermal diffusion within the bulk PCM can be a major challenge, leading to lower rates of heat output than can be achieved with encapsulated systems.

For domestic and small district water heating requirements, characterized by heating rates tipically below 20 kW, more complex heat exchanger configurations can be used to obtain higher

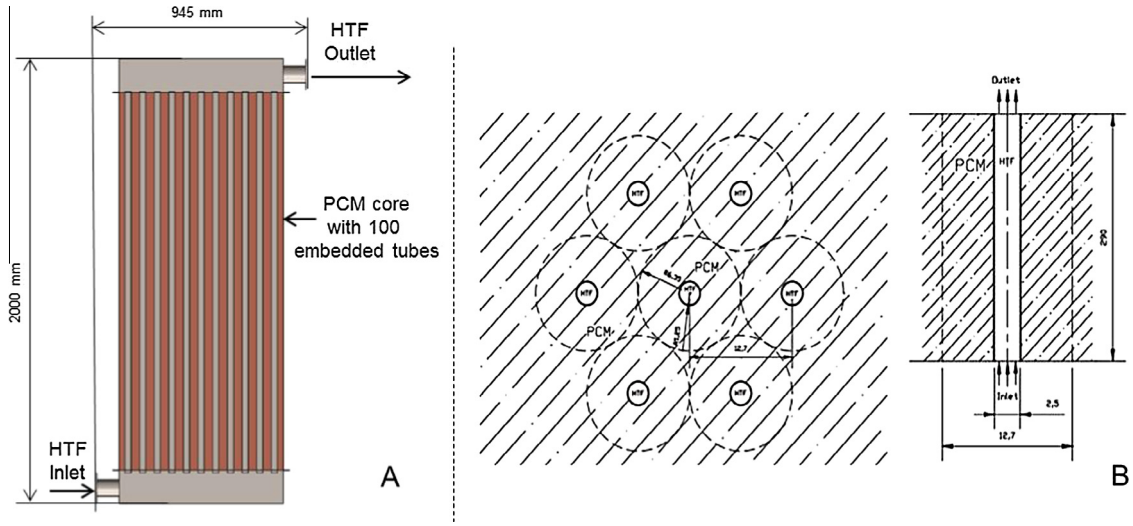

Fig. 7. Proposed design for a 827 L compact latent heat storage container for process heating applications (A), and the geometrical arrangement and tube spacing (B), studied by Colella et al. [12].

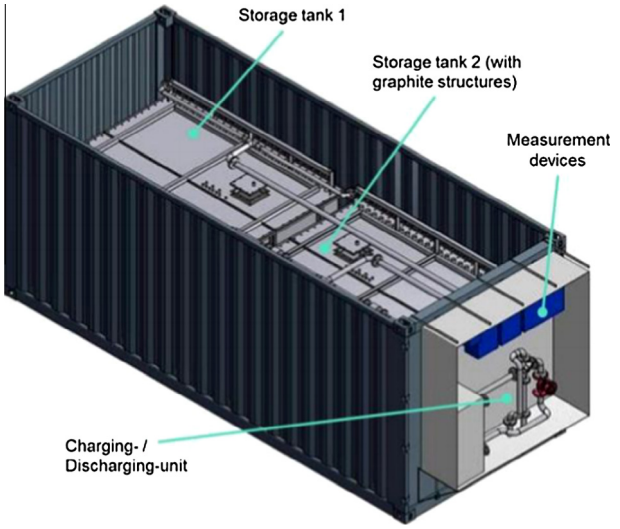

Fig. 8. Structure of the prototype storage system developed by Deckert et al. [87] to meet the heat demands of a district heating network.

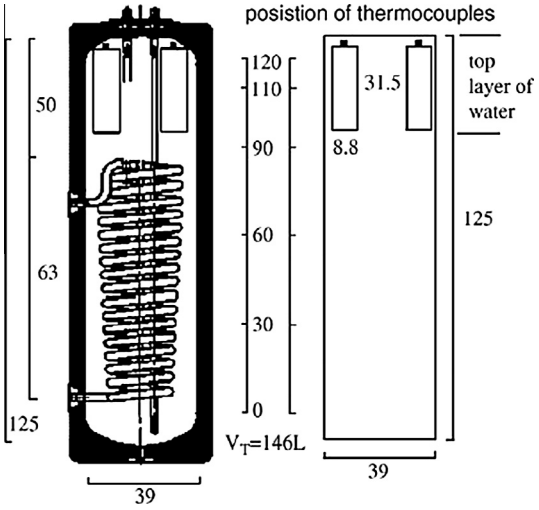

Fig. 9. Schematic representation illustrating the location of the encapsulated PCM modules inside the water tank of the experimental work undertaken by Cabeza et al. [89].

inlet–outlet temperature differentials, since flow head losses are not the main challenge. Fig. 6 presents a schematic diagram of a 18,770 L PCM container modelled by Nakaso et al. [18], with a predicted thermal storage capacity using a paraffin wax with a melting temperature of 49 °C (discharged from 53 °C to 40 °C) of 516.7 kW h_{th}. He predicted numerically that without any thermal enhancement, the system could provide a constant 25 kW thermal power output for 80% of its total capacity, around 16 h and 32 min.

For large process heating requirements, large parallel arrays of tubes should be used, to overcome the heat transfer limitation imposed by the PCMs low thermal conductivity [12], rather than using complex heat exchanging geometries [18]. This enables the heat transfer path length to be reduced, higher power outputs achieved, reduced heat transfer fluid volume flow rate, and lower frictional head losses. Fig. 7A, illustrates the cross section of a rectangular cross section container with 100 tubes running in parallel for the heat transfer fluid. The proposed system could contain up to 827 L of PCM within a container 2 m high with a square cross section of 800 mm × 800 mm.

Latent heat storage for use with district heating networks has been studied by Colella et al. [12], and compared to hot water storage which is commonly used in many district heating systems. Due to the high energy density of latent heat storage systems, portable containers charged from industrial waste heat streams could be of potential interest in providing heat to the nearby district heating networks. Fig. 8 presents the design of a prototype thermal storage system for use with a district heating system housed in a 20 foot long cargo container tested by Deckert et al. [87]; the system can store a maximum capacity of 1758 kW h_{th}, using sodium acetate trihydrate between 90 and 25 °C; being the heat supplied by a biogas plant located 6 km from the district heat network with the charged store being physically transported between locations. Limiting the practical storage capacity to 80%, the compact latent heat storage system could provide 40 kW of nearly constant thermal output over a discharge time of 38 h.

Systems using encapsulated PCMs offer higher heat transfer area per system volume [$m^2_{HT\ area}/m^3_{System}$], but have lower volumetric ratios [m^3_{PCM}/m^3_{sytem}]. Another advantage is the ease of obtaining

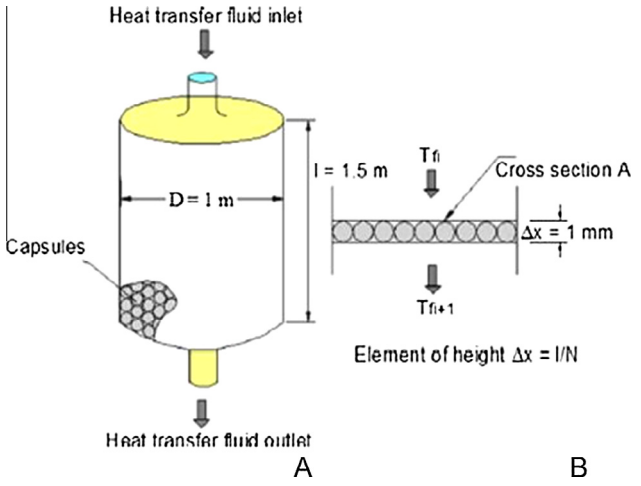

Fig. 10. Simplified drawing of the modelled container (A) and cross section view of a nodule (B) of the packed bed model used by Regin et al. [91].

leak-proof solutions [9], proving suitable for less stable materials. The ability to be used with any given storage container provides great versatility, regardless of size; hence their popularity [86,88].

The geometries used vary significantly with the application, but they commonly have cylindrical or spherically shaped capsules, which can be inserted into off the shelf storage containers. Cabeza et al. [89], undertook a study in which two to six small cylinders containing a mixture of 90% sodium acetate trihydrate +10% graphite as the PCM were inserted in the upper part of a domestic hot water tank, making good use of the tank's thermal stratification, Fig. 9. The study concluded that, by adding 2% by volume of PCM (2 tubes) to the top region of the store, they could achieve an increase of 40% in the thermal storage capacity; comparing to the common water tank over a temperature difference of 1 K where the PCM solidifies (around 54 °C).

Encapsulating a PCM into spherical capsules, Fig. 10, provides closer packing within the storage system [90]. This approach benefits from higher mixing of the heat transfer fluid and consequently better convective heat transfer coefficients [86] than in the vertical cylinders illustrated in Fig. 9. However, lower rates of thermal diffusion within the spherical capsules can reduce their effectiveness in exchanging heat to and from the heat transfer fluid [91].

Direct space cooling applications in which the charging of the store occurs during the night and discharge occurs during the day to cool office areas have been studied by Mosaffa et al. [92] and Jiao And Xu [93]. Air was used as the heat transfer fluid with the PCM encapsulated in rectangular cross section slabs with $CaCl_2 \cdot 6H_2O$ as PCM. Fig. 11 illustrates the modelled system studied by Mosaffa et al. [92] with a PCM store in an office air duct. The storage unit was composed by 80 rectangular slabs with 10 mm thickness, 500 mm width and 1.3 m length, with air gaps of 3.2 mm thickness. The modelling results demonstrated that the system could provide a constant heat output rate between 5 and 3 kW, with the air flow varying rate from 1600 to 800 m^3/h respectively; for an inlet air temperature of 36 °C, the system's predicted coefficient of performance was around 7.

Another possible application for an encapsulated latent heat storage system was studied in [94] and is illustrated in Fig. 12. Heat from solar thermal collectors is stored in an array of cylinders filled with paraffin wax, air is used as the heat transfer fluid. Due to the poor convective heat transfer obtained to the outer shell of the capsules, aluminium strips were used to increase the effective heat transfer area of the cylinders, providing a substantial increase in the latent heat storage system's effectiveness and the global solar collector system efficiency.

3.1.1. Micro encapsulation of PCM

Micro capsules with a diameter varying from around 1 to 1000 μm [32] have been used to encapsulate PCMs, such micro capsules when introduced into a liquid, form a slurry, effectively increasing the thermal storage capacity of the working fluid and potentially its convective heat transfer properties. Current production methods for micro encapsulated PCMs are: coacervation, suspension and emulsion polymerization, poly-condensation and polyadition. Huang et al. [21], undertook a study in which a cylindrical container filled with a PCM slurry was heated and cooled using a helical coil heat exchanger. The slurry varied between 25%, 35% and 50% composition by volume of PCM capsules to carrier fluid. It was concluded that higher volumetric ratios (50% respectively) reduced natural convection heat transfer within the storage container. Another characteristic of using PCM filled microcapsules was the low PCM volumetric ratios per capsule, normally around 50%, which when multiplied by the slurry volumetric ratio leads to a very low PCM volumetric ratio which reduces the typical heat capacity increase obtained when using PCMs.

3.2. Heat transfer enhancement methods

Most PCMs have low thermal conductivity, which can seriously affect the storage system charge and discharge rates. To address this limitation, extended metal surfaces [84], conductive powders [17] or conductive matrices [18] have proven to be effective in increasing the PCMs heat transport properties, leading to a more uniform temperature within the PCM and better charge and discharge effectiveness for the latent heat storage container/system.

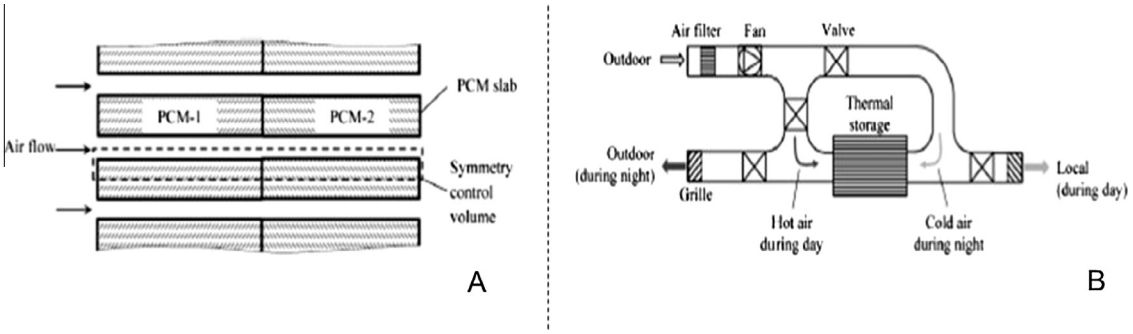

Fig. 11. Detailed view of the heat transfer arrangement inside the PCM module (A) and schematic representation of the container integration into the ventilation system studied by Mosaffa et al. [92].

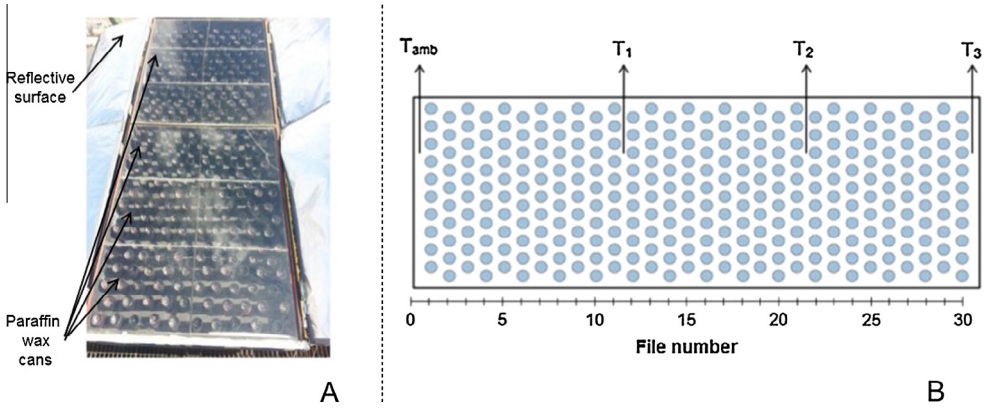

Fig. 12. Picture of the solar air absorber (A) and schematic diagram of the absorber presenting the thermocouple positions for the experimental work performed by Reyes et al. [94].

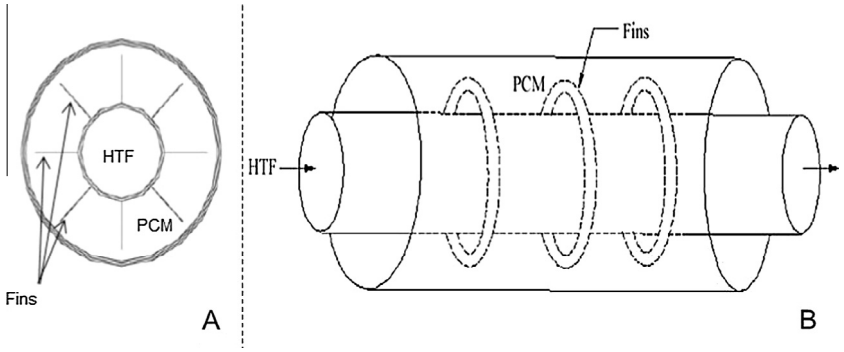

Fig. 13. Cross section of a tube in tube heat storage unit with longitudinal fins from Agyenim et al. [9], and a schematic representation of a tube in tube heat storage unit with annular fins from Jegadheeswaran et al. [17].

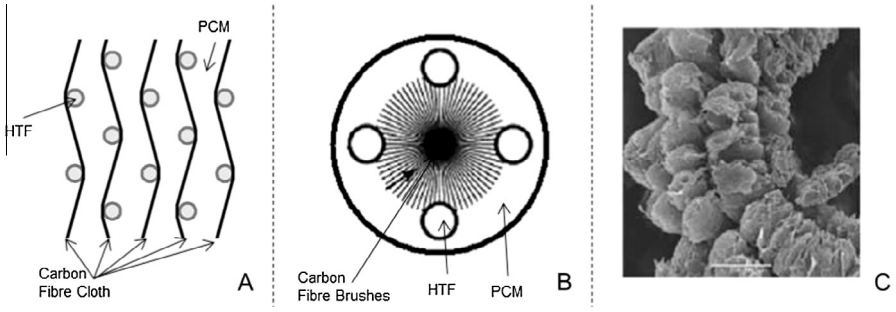

Fig. 14. Cross-section diagram of a carbon fibre cloth (A), a carbon fibre brush (B) and EG viewed with a SEM microscope Jegadheeswaran et al. [17].

3.2.1. Extended metal surfaces

One of the most widely used heat transfer enhancement techniques used is to increase the heat transfer area by adding extended metal surfaces, fins. Various studies have been made on modelling the phase change process with different fin geometries [95,96]. A study made by Agyenim et al. [9], tested a compact horizontal tube in tube container using erythritol as the PCM, using axial fins to enhance heat transfer. They found for this system melting/solidifying properties that would provide a suitable a heat source for driving an absorption cooling system. Fig. 13 illustrates two common fin geometries widely used in the literature [17].

3.2.2. Heat transfer enhancement using carbon

Exfoliated graphite, also known as expanded graphite (EG), with a thermal conductivity ranging from 24 to 470 W/m K, has the potential to increase the global PCM thermal conductivity [17], with low volume ratios (usually around 10–15% [32]). EG is generally obtained from the oxidation of natural graphite with a mixture of nitric and sulphuric acid, followed by drying in an oven and rapid heating in a furnace at 800–900 °C to obtain rapid expansion. The PCM is impregnated into the EG under vacuum, this prevents the formation of air gaps within the EG/PCM composite [43,17]. This technique is the most effective procedure currently used to enhance the PCM thermal conductivity [97]. It also provides a shape-stabilized (SS) form to the PCM since the pore cavities can withstand the thermal expansion typical during phase change and prevent leakage of molten PCM [43] (see Fig. 14).

The container studied by Nakaso et al. [18] presented in Fig. 6 was predicted to double its heat output (from 25 to 50 kW_{th}) if a carbon fibre cloth of 0.8% v/v was incorporated into the system. The system would then provide a nearly constant heat output of 50 kW for around 10 h and 20 min.

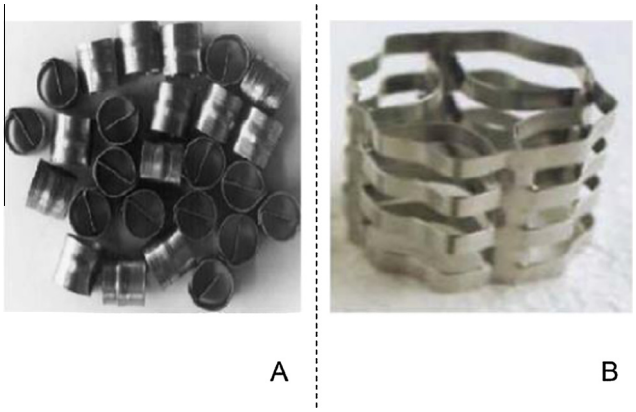

Fig. 15. Stainless steel (A) and aluminium lessing rings (B) from Agyenim et al. [9].

3.2.3. Thermal conductivity enhancement using metal matrices

Using sparse metal matrices is another effective way to increase thermal conductivity within a PCM container, structure that would also provide multiple nucleation points. Steel wool is a more feasible method of improving thermal conductivity of a PCM, compared to expandable graphite, but does not provide a shape stabilized solution; since it is not as compactable as graphite. Fig. 15 presents 2 approaches used to effectively enhance heat transfer within a PCM.

3.2.4. Using conductive powders

Including small percentages by volume of metallic particles (aluminium, copper, silver, nickel), or graphite [17] can also increase thermal diffusion within low thermal conductivity PCMs. It would also have the added benefit of increasing the number of potential nucleation points, potentially enhancing crystallization within the PCM. However, the conductive material could lose its miscibility when the PCM is in the molten state (due to differences in density), separating from the storage material and sinking to the base of the container. This could be prevented by including gelling agents in the PCM [43], with a consequent reduction in the PCM volume ratio.

3.2.5. Direct heat transfer techniques

Another technique to increase the heat transfer would be to provide direct contact between the heat transfer fluid and the PCM. This would provide an effective increase in heat transfer during the melting process since the convective nature of the heat transfer fluid would act directly on the solid PCM phase [20]. Wang et al. [22] studied the performance of a direct contact latent heat storage container using erythritol and an heat transfer oil, Fig. 16; and it concluded that at the beginning of the melt process the oil has a low flow rate due to the block of solid erythritol, the top surface of the PCM melts faster than the bottom due to the higher heat transfer rate and the melting time varies significantly with the oil flow rate.

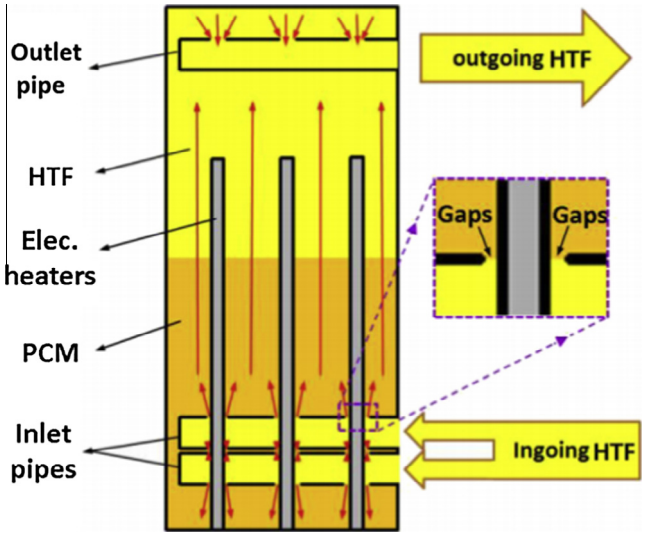

Fig. 17. Schematic cross section showing the locations of the electric heaters in the inlet pipes, studied by Guo et al. [23].

To overcome the initial blocking of the fluid flow path when the PCM is in the solid state, Guo et al. [23] studied the insertion of electric heaters, Fig. 17, and concluded that the overall energy spent on melting the initial flow pathways was 5% of the total thermal energy stored.

4. Conclusions

Phase change materials have the potential to store large amounts of energy within a smaller temperature range when compared to common sensible heat storage materials. Due to the low thermal conductivities of many PCMs, poor rates of thermal diffusion within the PCM can seriously affect the storage system charge and discharge rates that can be achieved.

A comprehensive review of PCMs melting between 0 and 250 °C has been made and the thermophysical properties of the materials having the most appropriate properties presented. Below 100 °C, organic compounds and salt hydrates are the most interesting materials. Eutectic mixtures with Urea seem promising around

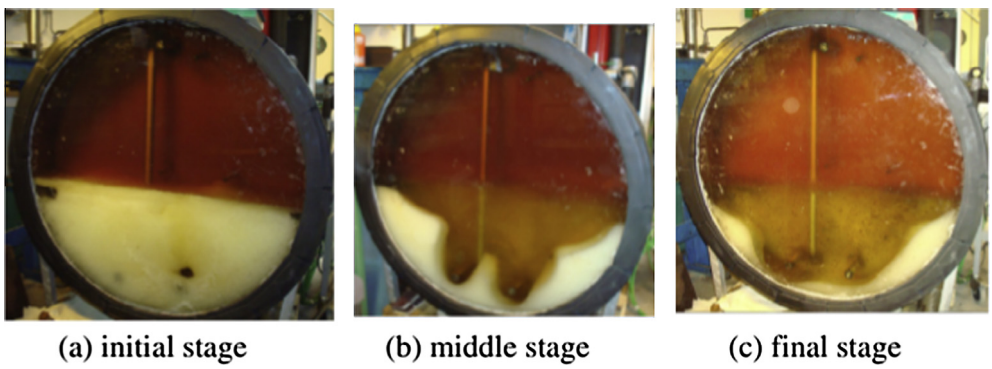

Fig. 16. Temporal variation of the melting process in a direct contact heat transfer container using erythritol as the PCM and oil as the heat transfer fluid, from Wang et al. [20].

100 °C, and in the range from 130 °C up to 1250 °C eutectic mixtures of inorganic salts appear the most promising PCMs. A mixture of sodium and potassium fomates melting around 170 °C appears attractive due to is relatively low price and moderate latent heat of fusion.

A review of potential indirect latent heat storage containers and systems suitable for integration with various process heating and cooling networks is also reported. Due to its geometrical versatility, encapsulated systems seem more feasible since they can be integrated to any existing system without major technical constrains, although they have lower PCM volume ratios. Compact systems offer larger isothermal stages due to their higher PCM volume ratios; however, heat transfer enhancement among the PCM is imperative to achieve reasonable thermal power output rates, since PCMs thermal conductivity can be a major issue.

Acknowledgements

The research presented in this paper is funded by the EPSRC through Grant reference EP/K011847/1, Interdisciplinary centre for Storage, Transformation and Upgrading of Thermal Energy (i-STUT)E and a Loughborough University funded PhD studentship.

References

[1] International Energy Agency. World energy outlook 2013; 2015.
[2] Harris K, Annut A, MacLeay I. Digest of United Kingdom energy statistics, 2015, https://www.gov.uk/government/uploads/system/uploads/attachment_data/file/450302/DUKES_2015.pdf.
[3] Hawkes AD. Long-run marginal CO_2 emissions factors in national electricity systems. Appl Energy 2014;125(July):197–205.
[4] Hawkes AD. Estimating marginal CO_2 emissions rates for national electricity systems. Energy Pol. 2010;38(10):5977–87.
[5] National grid. UK future energy scenarios 2014. Energy, no. July; 2014. p. 220.
[6] Haillot D, Franquet E, Gibout S, Bédécarrats J-P. Optimization of solar DHW system including PCM media. Appl Energy 2013;109(September):470–5.
[7] Ibáñez M, Cabeza LF, Solé C, Roca J, Nogués M. Modelization of a water tank including a PCM module. Appl Therm Eng 2006;26:1328–33.
[8] Zondag H, Kikkert B, Smeding S, de Boer R, Bakker M. Prototype thermochemical heat storage with open reactor system. Appl Energy 2013;109(September):360–5.
[9] Agyenim F, Hewitt N, Eames P, Smyth M. A review of materials, heat transfer and phase change problem formulation for latent heat thermal energy storage systems (LHTESS). Renew Sustain Energy Rev 2010;14:615–28.
[10] Gil A, Oró E, Peiró G, Álvarez S, Cabeza LF. Material selection and testing for thermal energy storage in solar cooling. Renew Energy 2013;57:366–71.
[11] Gil A, Barreneche C, Moreno P, Solé C, Inés Fernández A, Cabeza LF. Thermal behaviour of d-mannitol when used as PCM: comparison of results obtained by DSC and in a thermal energy storage unit at pilot plant scale. Appl Energy 2013;111(November):1107–13.
[12] Colella F, Sciacovelli A, Verda V. Numerical analysis of a medium scale latent energy storage unit for district heating systems. Energy 2012;45(1):397–406.
[13] Kensby J, Trüschel A, Dalenbäck J-O. Potential of residential buildings as thermal energy storage in district heating systems – results from a pilot test. Appl Energy 2015;137(January):773–81.
[14] Vivian J, Manente G, Lazzaretto A. A general framework to select working fluid and configuration of ORCs for low-to-medium temperature heat sources. Appl Energy 2015;156(October):727–46.
[15] Higgo AR, Zhang TJ. Characterization of a compact organic rankine cycle prototype for low-grade transient solar energy conversion. Energy Proc 2015;69(May):1113–22.
[16] Kalogirou S. The potential of solar industrial process heat applications. Appl Energy 2003;76(4):337–61.
[17] Jegadheeswaran S, Pohekar SD. Performance enhancement in latent heat thermal storage system: a review. Renew Sustain Energy Rev 2009;13(9):2225–44.
[18] Nakaso K, Teshima H, Yoshimura A, Nogami S, Hamada Y, Fukai J. Extension of heat transfer area using carbon fiber cloths in latent heat thermal energy storage tanks. Chem Eng Process Process Intensif 2008;47(5):879–85.
[19] Qi GQ, Liang CL, Bao RY, Liu ZY, Yang W, Xie BH, et al. Polyethylene glycol based shape-stabilized phase change material for thermal energy storage with ultra-low content of graphene oxide. Sol Energy Mater Sol Cells 2014;123:171–7.
[20] Wang W, Yang X, Fang Y, Ding J, Yan J. Preparation and thermal properties of polyethylene glycol/expanded graphite blends for energy storage. Appl Energy 2009;86(9):1479–83.
[21] Huang MJ, Eames PC, McCormack S, Griffiths P, Hewitt NJ. Microencapsulated phase change slurries for thermal energy storage in a residential solar energy system. Renew Energy 2011;36:2932–9.
[22] Wang W, He S, Guo S, Yan J, Ding J. A combined experimental and simulation study on charging process of Erythritol–HTO direct-blending based energy storage system. Energy Convers Manage 2014;83(July):306–13.
[23] Guo S, Zhao J, Wang W, Jin G, Wang X, An Q, et al. Experimental study on solving the blocking for the direct contact mobilized thermal energy storage container. Appl Therm Eng 2015;78(March):556–64.
[24] Johansson I. AMIDES, fatty acid. Kirch-Othmer Encycl Ind Chem; 2000.
[25] Raemy A, Schweizer TF. Thermal behaviour of carbohydrates studied by heat flow calorimetry. J Therm Anal 1983;28:95–108.
[26] Schiweck H, Bär A, Vogel R, Schwarz E, Kunz M, Dusautois C, et al. Sugar alcohols. In: Ullmann's encylcopedia of industrial chemistry. Wiley-VCH Verlag GmbH & Co; 2012. p. 2–32.
[27] Cornils B, Lappe P. Dicarboxylic acids aliphatic. In: Ullmann's encyclopedia of industrial chemistry. Wiley-VCH Verlag GmbH & Co. KGaA; 2008.
[28] Kerridge DH. The chemistry of molten acetamide and acetamide complexes. Chem Soc Rev 1988;17:181.
[29] Kenisarin MM. Thermophysical properties of some organic phase change materials for latent heat storage. A review. Sol Energy 2014;107:553–75.
[30] Mavrovic I, Shirley AR, Coleman GR. Urea, vol. 2. Kirk-Othmer Encycl Chem Technol; 2010. p. 1–21.
[31] Haillot D, Bauer T, Kröner U, Tamme R. Thermal analysis of phase change materials in the temperature range 120–150 °C. Thermochim Acta 2011;513(1–2):49–59.
[32] Jankowski NR, McCluskey FP. A review of phase change materials for vehicle component thermal buffering. Appl Energy 2014;113:1525–61.
[33] Miller AP. Lange's handbook of chemistry. Am J Pub Heal Nations Heal 1941;31(12):1324.
[34] Harish S, Orejon D, Takata Y, Kohno M. Thermal conductivity enhancement of lauric acid phase change nanocomposite with graphene nanoplatelets. Appl Therm Eng 2015;80(April):205–11.
[35] Yuan Y, Zhang N, Tao W, Cao X, He Y. Fatty acids as phase change materials: a review. Renew Sustain Energy Rev 2014;29:482–98.
[36] Tang F, Cao L, Fang G. Preparation and thermal properties of stearic acid/titanium dioxide composites as shape-stabilized phase change materials for building thermal energy storage. Energy Build 2014;80(September):352–7.
[37] Farid MM, Khudhair AM, Razack SAK, Al-Hallaj S. A review on phase change energy storage: materials and applications. Energy Convers Manage 2004;45:1597–615.
[38] Silakhori M, Fauzi H, Mahmoudian MR, Metselaar HSC, Mahlia TMI, Khanlou HM. Preparation and thermal properties of form-stable phase change materials composed of palmitic acid/polypyrrole/graphene nanoplatelets. Energy Build 2015;99(July):189–95.
[39] Website of Rubitherm GmbH. Rubitherm GmbH; 2016. <http://www.rubitherm.eu/>.
[40] Dunn JG, Smith HG, Willix RL. The supercooling of acetamide. Thermochim Acta 1984;80(2):343–53.
[41] Riemensschneider W, Tanifuji M. Oxalic acid. In: Ullmann's encyclopedia of industrial chemistry. Wiley-VCH Verlag GmbH & Co. KGaA; 2012. p. 543–600.
[42] Tong B, Tan ZC, Zhang JN, Wang SX. Thermodynamic investigation of several natural polyols (III): heat capacities and thermodynamic properties of erythritol. J Therm Anal Calorim 2009;95(2):469–75.
[43] Pielichowska K, Pielichowski K. Phase change materials for thermal energy storage. Prog Mater Sci 2014;65:67–123.
[44] Lorz P, Towae F, Enke W, Jäckh R, Bhargava N, Hillesheim W. Phthalic acid and derivates. In: Ullmann's encyclopedia of industrial chemistry. Wiley-VCH Verlag GmbH & Co KGaA; 2012. p. 35–154.
[45] Muraishi K, Suzuki Y. The thermal behaviour of dicarboxylic acids in various atmospheres. Thermochim Acta 1994;232:195–203.
[46] Lohbeck K, Haferkorn H, Fuhrmann W, Fedtke N. Maleic and fumaric acids. In: Ullmann's encyclopedia of industrial chemistry. Wiley-VCH Verlag GmbH & Co. KGaA; 2005. p. 413–54.
[47] Felthouse T, Burnett J, Horrell B, Mommey M, Kuo Y-J, et al. Maleic anhydride, maleic acid, and fumaric acid. In: Kirk-Othmer encyclopedia of industrial chemistry. John Wiley & Sons, Inc.; 1933. no. 10.
[48] Maki T, Takeda K. Benzoic acid and derivatives. Ullmann's encyclopedia of industrial chemistry, vol. 60. p. 329–42.
[49] Hasl T, Jiricek I. The prediction of heat storage properties by the study of structural effect on organic phase change materials. Energy Proc 2014;46:301–9.
[50] Barone G, Della Gatta G, Ferro D, Piacente V. Enthalpies and entropies of sublimation, vaporization and fusion of nine polyhydric alcohols. J Chem Soc Faraday Trans 1990;86(1):75.
[51] Solé A, Neumann H, Niedermaier S, Martorell I, Schossig P, Cabeza LF. Stability of sugar alcohols as PCM for thermal energy storage. Sol Energy Mater Sol Cells 2014;126:125–34.
[52] Krishna Bama G, Anitha R, Ramachandran K. On the thermal properties of aqueous solution of D-mannitol. Nondestruct Test Eval 2009;25(1):67–75.
[53] Gil A, Oró E, Miró L, Peiró G, Ruiz Á, Salmerón JM, et al. Experimental analysis of hydroquinone used as phase change material (PCM) to be applied in solar cooling refrigeration. Int J Refrig 2014;39(March):95–103.
[54] Lane GA. Phase change materials for energy storage nucleation to prevent supercooling. Sol Energy Mater Sol Cells 1992;27:135–60.

[55] Habashy GM, Kolta GA. Thermal decomposition of the hydrates of barium hydroxide. J Inorg Nucl Chem 1972;34(1961):57–67.
[56] Porisini FC. Salt hydrates used for latent heat storage: corrosion of metals and reliability of thermal performance. Sol Energy 1988;41(2):193–7.
[57] Acree WE. Thermodynamic properties of organic compounds: enthalpy of fusion and melting point temperature compilation. Thermochim Acta 1991;189:37–56.
[58] Zalba B. Review on thermal energy storage with phase change: materials, heat transfer analysis and applications. Appl Therm Eng 2003;23(3):251–83.
[59] Hadjieva M, Stoykov R, Filipova T. Composite salt-hydrate concrete system for building energy storage. Renew Energy 2000;19(1–2):111–5.
[60] Sandnes B, Rekstad J. Supercooling salt hydrates: stored enthalpy as a function of temperature. Sol Energy 2006;80(5):616–25.
[61] Johansen JB, Dannemand M, Kong W, Fan J, Dragsted J, Furbo S. Thermal conductivity enhancement of sodium acetate trihydrate by adding graphite powder and the effect on stability of supercooling. Energy Proc 2015;70 (May):249–56.
[62] Patnaik P. Handbook of inorganic chemicals. McGraw-Hill; 2003.
[63] Zhongliang L, Chongfang M, Jing L. An experimental study on the stability and reliability of the thermal properties of barium hydroxide octahydrate as a phase change material. In: Proc 7th expert meet work IEA annex 17 Adv Therm Energy Storage through Phase Chang Mater Chem React – Feasibility Stud Demonstr Proj; 2004. p. 63–9.
[64] Pilar R, Svoboda L, Honcova P, Oravova L. Study of magnesium chloride hexahydrate as heat storage material. Thermochim Acta 2012;546:81–6.
[65] Bauer T, Laing D, Tamme R. Recent progress in alkali nitrate/nitrite developments for solar thermal power applications. Molten Salts Chem Technol 2011(June):1–10.
[66] Gomez JC, Calvet N, Starace AK, Glatzmaier GC. $Ca(NO_3)_2$–$NaNO_3$–KNO_3 molten salt mixtures for direct thermal energy storage systems in parabolic trough plants. J Sol Energy Eng 2013;135(May):021016.
[67] Cordaro JG, Rubin NC, Bradshaw RW. Multicomponent molten salt mixtures based on nitrate/nitrite anions. J Sol Energy Eng 2011;133(February):011014.
[68] Yamada M, Tago M, Fukusako S, Horibe A. Melting point and supercooling characteristics of molten salt. Thermochim Acta 1993;218(May):401–11.
[69] Rowlinson J. Molecular thermodynamics of fluid-phase equilibria. J Chem Thermodyn 1970;2(1):158–9.
[70] Yanping Y, Wenquan T, Xiaoling C, Li B. Theoretic prediction of melting temperature and latent heat for a fatty acid eutectic mixture. J Chem Eng Data 2011;56(6):2889–91.
[71] Gmehling J, Li J, Schiller M. A modified UNIFAC model. 2. Present parameter matrix and results for different thermodynamic properties. Ind Eng Chem Res 1993;32(1):178–93.
[72] Diarce G, Gandarias I, Campos-Celador Á, García-Romero A, Griesser UJ. Eutectic mixtures of sugar alcohols for thermal energy storage in the 50–90 °C temperature range. Sol Energy Mater Sol Cells 2015;134(March):215–26.
[73] Sharma A, Tyagi VV, Chen CR, Buddhi D. Review on thermal energy storage with phase change materials and applications. Renew Sustain Energy Rev 2009;13:318–45.
[74] Baran G, Sari A. Phase change and heat transfer characteristics of a eutectic mixture of palmitic and stearic acids as PCM in a latent heat storage system. Energy Convers Manage 2003;44(20):3227–46.
[75] Olivares RI, Edwards W. $LiNO_3$–$NaNO_3$–KNO_3 salt for thermal energy storage: thermal stability evaluation in different atmospheres. Thermochim Acta 2013;560:34–42.
[76] Roget F, Favotto C, Rogez J. Study of the KNO_3–$LiNO_3$ and KNO_3–$NaNO_3$–$LiNO_3$ eutectics as phase change materials for thermal storage in a low-temperature solar power plant. Sol Energy 2013;95:155–69.
[77] Gamataeva BY, Bagomedova RM, Gasanaliev aM. Differentiation of the Li, Na, K||NO_2, NO_3 quaternary reciprocal system and phase formation in its stable partitioning tetrahedron $LiNO_2$–$NaNO_2$–KNO_2–KNO_3. Russ J Inorg Chem 2014;59(2):134–40.
[78] Janz GJ, Tomkins RPT. Molten salts: volume 5, Part 2. Additional single and multi-component salt systems. Electrical conductance, density, viscosity and surface tension data. New York; 1983.
[79] Gasanaliev AM, Gamataeva BY. Heat-accumulating properties of melts. Russ Chem Rev 2007;69:179–86.
[80] Dante L, Mario B, Augusto C, Paolo F. Molten mixtures of K, Na formates with alkali halides. Note I. Zeitschrift für Naturforschung A 1970;25:52.
[81] Kenisarin MM. High-temperature phase change materials for thermal energy storage. Renew Sustain Energy Rev 2010;14:955–70.
[82] Janz GJ, Tomkins RPT. Molten salts: volume 5, part 1 additional single and multi-component salt systems. Electrical conductance, density, viscosity and surface tension data. New York; 1980.
[83] Hewitt NJ. Heat pumps and energy storage – the challenges of implementation. Appl Energy 2012;89(1):37–44.
[84] Agyenim F, Eames P, Smyth M. Experimental study on the melting and solidification behaviour of a medium temperature phase change storage material (Erythritol) system augmented with fins to power a $LiBr/H_2O$ absorption cooling system. Renew Energy 2011;36(1):108–17.
[85] Trp A. An experimental and numerical investigation of heat transfer during technical grade paraffin melting and solidification in a shell-and-tube latent thermal energy storage unit. Sol Energy 2005;79(6):648–60.
[86] Barba a, Spiga M. Discharge mode for encapsulated PCMs in storage tanks. Sol Energy 2003;74(February):141–8.
[87] Deckert M, Scholz R, Binder S, Hornung A. Economic efficiency of mobile latent heat storages. Energy Proc 2014;46:171–7.
[88] a Hawlader MN, Uddin MS, Zhu HJ. Encapsulated phase change materials for thermal energy storage: experiments and simulation. Int J Energy Res 2001;26 (January):159–71.
[89] Cabeza LF, Ibanez M, Sole C, Roca J, Nogues M. Experimentation with a water tank including a PCM module. Sol Energy Mater Sol Cells 2006;90(9):1273–82.
[90] Wu M, Xu C, He Y-L. Dynamic thermal performance analysis of a molten-salt packed-bed thermal energy storage system using PCM capsules. Appl Energy 2014;121(May):184–95.
[91] Regin A Felix, Solanki SC, Saini JS. An analysis of a packed bed latent heat thermal energy storage system using PCM capsules: numerical investigation. Renew Energy 2009;34(7):1765–73.
[92] Mosaffa AH, Garousi Farshi L, Infante Ferreira CA, Rosen MA. Energy and exergy evaluation of a multiple-PCM thermal storage unit for free cooling applications. Renew Energy 2014;68(August):452–8.
[93] Jiao F, Xu P. Simulation and feasibility analysis of PCM based passive cooling technique in residential house. Proc Eng 2015;121:1969–76.
[94] Reyes A, Henríquez-Vargas L, Aravena R, Sepúlveda F. Experimental analysis, modeling and simulation of a solar energy accumulator with paraffin wax as PCM. Energy Convers Manage 2015;105(November):189–96.
[95] Shon J, Kim H, Lee K. Improved heat storage rate for an automobile coolant waste heat recovery system using phase-change material in a fin–tube heat exchanger. Appl Energy 2014;113(January):680–9.
[96] Sciacovelli A, Gagliardi F, Verda V. Maximization of performance of a PCM latent heat storage system with innovative fins. Appl Energy 2015;137 (January):707–15.
[97] Merlin K, Delaunay D, Soto J, Traonvouez L. Heat transfer enhancement in latent heat thermal storage systems: comparative study of different solutions and thermal contact investigation between the exchanger and the PCM. Appl Energy 2016;166(March):107–16.